International Journal of Pharmaceutics 693 (2026) 126680

Contents lists available at ScienceDirect

International Journal of Pharmaceutics

journal homepage: www.elsevier.com/locate/ijpharm

Raman-assessed cutaneous pharmacokinetics of doxepin topical products☆

Panagiota Zarmpi [a,b], Dimitrios Tsikritsis [c], Natalie A. Belsey [b,c], Elena Rantou [d], Priyanka Ghosh [e], Annette L. Bunge [f], Andrew C. Watson [a], Timothy J. Woodman [a], M. Begoña Delgado-Charro [a], Richard H. Guy [a,*]

[a] University of Bath, Department of Life Sciences, Claverton Down, Bath BA2 7AY, UK
[b] University of Surrey, School of Chemistry & Chemical Engineering, Guildford GU2 7XH, UK
[c] National Physical Laboratory, Teddington TW11 0LW, UK
[d] Office of Biostatistics, Office of Translational Sciences, Center for Drug Evaluation and Research, U.S. Food and Drug Administration, White Oak Campus, Silver Spring, MD 20993, USA
[e] Office of Research and Standards, Office of Generic Drugs, Center for Drug Evaluation and Research, U.S. Food and Drug Administration, White Oak Campus, Silver Spring, MD 20993, USA
[f] Colorado School of Mines, Department of Chemical & Biological Engineering, Golden, CO 80401, USA

ARTICLE INFO

Keywords:
Raman spectroscopy
Cutaneous pharmacokinetics
Topical drug bioavailability
Topical drug product bioequivalence
Regulatory science

ABSTRACT

Development of regulatory science tools to facilitate and accelerate accessibility to complex generic drug products continues to be the focus of significant research activity. The application of confocal Raman spectroscopy to the assessment of cutaneous drug pharmacokinetics is a particular example and has been exploited here to compare two approved topical creams (the reference-listed drug product and a generic) of doxepin hydrochloride with an intentionally non-equivalent, laboratory-made solution of the drug. Experiments involved administration of the formulations to pig skin *ex vivo* for 6 or 12 h (the uptake phase) followed by 2 and 4 h of clearance to generate Raman-assessed absorption-elimination profiles at nominal depths of 5 μm and 25 μm into the skin. This was achieved, despite overlap between spectral features of the drug with those from the skin, using a background signal removal strategy that also allowed the two functional excipients of the laboratory-made solution to be independently tracked. The areas under the Raman signal versus time absorption-elimination profiles showed (as expected) that the two creams were very similar but that the laboratory-made solution was distinctly different. First-order elimination rate constants describing the clearance phase post-application of doxepin from the superficial skin layers into the deeper tissue were also derived from the spectral data. While the experimental design was insufficiently powered to assess bioequivalence, the data background signal separation paradigm notably expands the potential value of the approach to a broader range of chemical species than had been originally envisaged.

1. Introduction

Regulatory science research, targeted at the development and validation of tools that can be used to establish the bioequivalence (BE) of a complex generic drug product to a reference-listed drug (RLD), has intensified over the past several years (Raney and Luke, 2020; Ghosh et al., 2022; Raney et al., 2022). With respect to products intended to treat dermatological disease after topical application to the skin, several complementary approaches to assess cutaneous pharmacokinetics have been identified and, to different extents, are being optimised (Food & Drug Administration (FDA), 2025). Vibrational spectroscopy, and Raman in particular, is one example that has attracted significant recent interest, not least because of its translational potential to essentially noninvasive *in vivo* use (Caspers et al., 2019; Nico et al., 2024; Pot et al., 2016).

Despite initial questions as to whether Raman would be sufficiently sensitive to quantify cutaneous drug bioavailability (BA) (Maciel Tabosa et al., 2022), the literature now provides evidence that the technique has been validated across a number of orthogonal, yet complementary approaches – including *in vitro* permeation testing, stratum corneum

☆ This article is part of a special issue entitled: 'Joke Bouwstra_IJP' published in International Journal of Pharmaceutics.

* Corresponding author.
E-mail address: r.h.guy@bath.ac.uk (R.H. Guy).

https://doi.org/10.1016/j.ijpharm.2026.126680
Received 19 November 2025; Received in revised form 24 January 2026; Accepted 12 February 2026
Available online 18 February 2026

sampling (tape-stripping) and mass spectrometry (Iliopoulos et al., 2020; Krombholz et al., 2022; Kourbaj et al., 2023; Maciel Tabosa et al., 2023; Belsey et al., 2023; Zarmpi et al., 2024) – and has achieved a number of key milestones. Firstly, the IR-silent region of the skin's spectrum (~1800–2500 cm^{-1}) has been exploited to show that Raman vibrational signals from compounds containing C≡N (4-cyanophenol, crisaborole) and C≡C (Janus kinase inhibitors, tazarotene) functional groups can be easily distinguished from any endogenous background and – in confocal mode – detected at skin depths well into the living epidermis (where many sites of pharmacological action are found) (Maciel Tabosa et al., 2023; Zarmpi et al., 2023; Jung et al., 2022). Secondly, the attenuation of Raman signals with increasing depth into the skin can be successfully normalised by simultaneously measuring the relatively constant Amide I signal (~1650 cm^{-1}) (Zarmpi et al., 2023). Confirmation and verification of these initial achievements were subsequently reported using stimulated Raman scattering (SRS) (Zarmpi et al., 2024) and a correlation methodology combining SRS with mass spectrometry (Belsey et al., 2023). Thirdly, in a major step forward, depth-resolved quantification of drugs detectable only within the 'fingerprint' region of the skin spectrum has been accomplished by applying a deconvolution–unmixing approach that both extracted the drug's true signal from the endogenous background and ensured that the data surpassed the critical level of detection. This was demonstrated in a confocal Raman study of metronidazole (MTZ) delivery from three commercial gels and two laboratory-made solutions, from which cutaneous pharmacokinetic metrics were extracted and then used to assess BE (Zarmpi et al., 2025). Finally, while vibrational spectroscopies have been shown to have the potential to track drug distribution post-application of complex topical products (for example, creams that often contain excipients that mask or supress Raman signals) (Iliopoulos et al., 2024), the necessary degree of sensitivity has yet to be generally established.

That said, the possibility that Raman may offer an essentially noninvasive regulatory science tool with which to establish topical product BE is very much 'on the radar' of the FDA and the European Medicines Agency (EMA). This is evidenced by the targeted research funding provided by the former's Office of Generic Drugs (FDA, 2025) and the latter's recently published guideline on quality and equivalence of locally applied, locally acting cutaneous products (EMA, 2025) which, while noting that more work is necessary before Raman can be given more serious consideration, nonetheless acknowledges its future potential.

Here, the utility 'bar' for Raman to overcome is further raised and used to compare two doxepin hydrochloride (DOX) products (RLD and approved generic for the treatment of itchy skin in adults with eczema or other skin conditions leading to repeated scratching) and a laboratory-made solution of the drug. The additional challenges addressed, therefore, are three-fold: (a) the products are creams, rather than the simpler – compositionally and spectrally – aqueous gels used in the MTZ investigation, (b) the most intense DOX signals overlap with the skin spectrum and, specifically, with that of Amide I meaning that depth normalisation has to use the alternative phenyl ring breathing signal at 1003 cm^{-1}, and (c) DOX is less skin permeable than MTZ making its detection with Raman more difficult.

2. Materials and methods

2.1. Materials

Doxepin hydrochloride (DOX, structure shown in Fig. 1) was purchased from MedChem Express (Princeton, NJ, USA). Dodecan-1-ol and polyethylene glycol (MW = 400) (PEG-400) were from Thermo Scientific (Leicestershire, UK). Propylene glycol (PG), polyethylene glycol (MW = 200) (PEG-200), polyethylene glycol 350 monomethyl ether (PEG-350), oleic acid, isopropyl myristate, isopropyl palmitate, and other solvents and chromatography reagents were acquired from Sigma

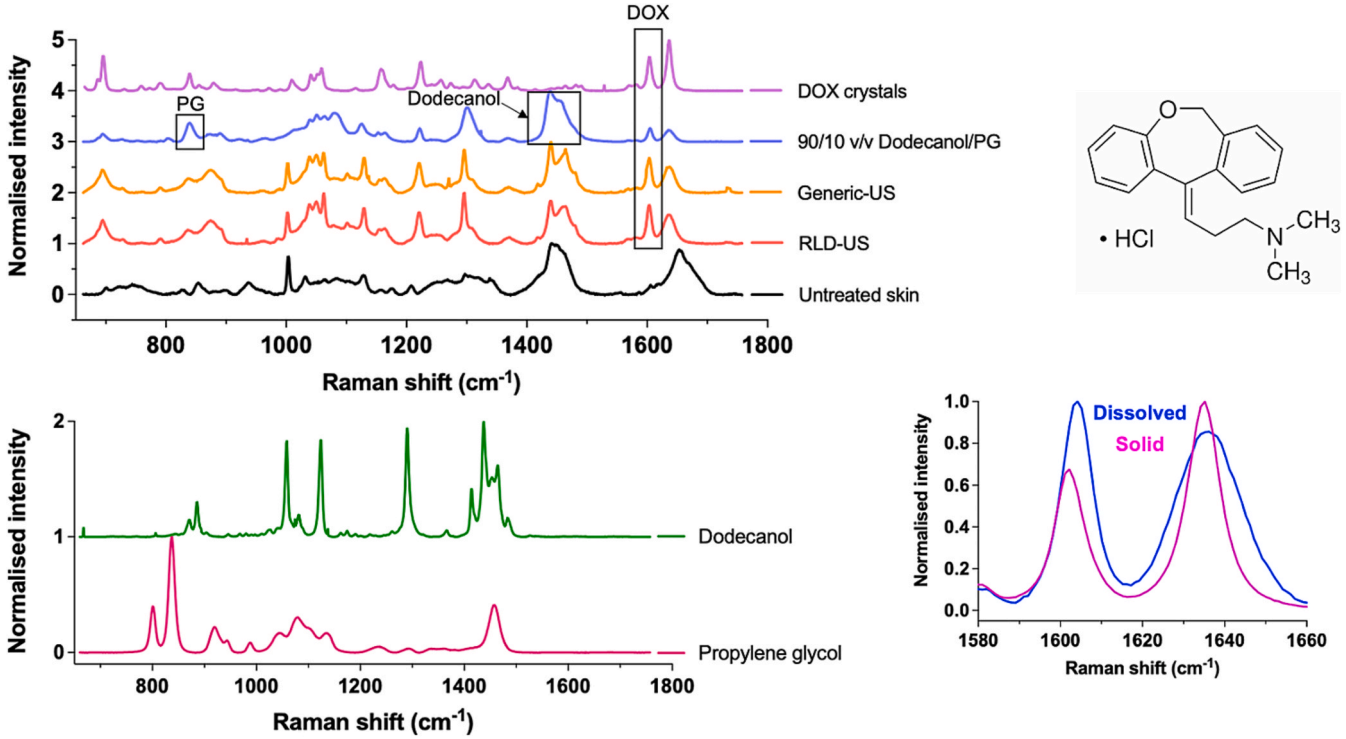

Fig. 1. Left panels – reference spectra (normalised by observed maximum intensity) of solid doxepin hydrochloride (DOX) (structure on the right (ChemDraw Professional 18.1.0.535, PerkinElmer, Waltham, MA, US)), PG, dodecanol, a saturated solution of DOX in dodecanol/PG, two commercial creams, and untreated skin. Lower right panel – Raman C=C stretching band of the aromatic ring (1605 cm^{-1}) and conjugated aromatic rings (1634 cm^{-1}) from dissolved and solid DOX (again normalised by maximum intensity).

Aldrich (Gillingham, Dorset, UK). Agar powder was from Merck (Darmstadt, Germany). Two approved and marketed (5% w/w) DOX topical cream products (Mylan Pharmaceutical Inc., Morgantown, WV, USA (NDC code 0378-8117-45) and Amneal Pharmaceuticals LLC, Bridgewater, NJ, USA (NDC code 69238-1733-6)) were purchased from WEP Clinical (Morrisville, NC, USA). Abdominal pig skin from three different animals was sourced from a tissue supplier and dermatomed (Zimmer®, Hudson, OH, USA) to a nominal thickness of 750 μm within 48 h post-slaughter. Visible hairs were carefully trimmed with scissors, and the tissue was stored at −20°C until thawed (~30 min at room temperature) just prior to use.

2.2. Solubility of doxepin hydrochloride

The solubility of DOX in various solvents and solvent mixtures – most of which are common in topical products – was measured using the shake-flask method (OECD, 1995). The solvents were phosphate-buffered saline pH 7.4 (PBS), PG, PEG-400, PEG-200, PEG-350 monomethyl ether, dodecanol, oleic acid, isopropyl myristate, and isopropyl palmitate; solvent mixtures (all 90/10 v/v) were PEG-200/dodecanol, PEG-350 monomethyl ether/PG, oleic acid/PG, and dodecanol/PG. Briefly, excess solid was introduced into glass vials (screw neck vial, 13 mm thread, 4 mL volume; Fischerbrand, Loughborough Leicestershire, UK) with 1 mL of each solvent/solvent mixture. The vials were tightly capped and placed in a shaking water bath (Fischer Scientific, Waltham, MA, USA) thermostatted at 32°C. After 24 h, samples were withdrawn, filtered (4-mm diameter, 0.45-μm pore size regenerated cellulose filters; SMI-LabHut Ltd, Maisemore, UK), diluted (if and as required) in methanol and analysed by HPLC-UV. All solubility measurements were performed in triplicate.

2.3. Doxepin hydrochloride formulations

The composition of the formulations selected for investigation are in Table 1. The cream from Mylan Pharmaceutical Inc. is the RLD in the US (and hereinafter designated RLD-US) and the cream from Amneal Pharmaceuticals is an FDA-approved generic (Generic-US) and considered bioequivalent to RLD-US. A saturated DOX solution in 90/10 v/v dodecanol/PG was chosen as a formulation unlikely to be bioequivalent (i.e., a negative control) to the RLD-US; the potential skin penetration enhancement of the fatty-alcohol/cosolvent excipient combination (Herkenne et al., 2008) plus the maximal thermodynamic activity of the drug were expected to optimise DOX uptake and delivery and to have higher bioavailability, compared to the commercial products.

2.4. Ex vivo evaluation of DOX uptake into and clearance from the skin

The DOX creams were applied at 20 mg cm^{-2}, the laboratory-made formulation at 150 μL cm^{-2}, to a 2.01 cm^2 area of abdominal pig skin mounted in a vertical Franz diffusion cell (PermeGear, Inc., Bethlehem, PA, USA). The amounts of cream and solution administered were close to those used clinically and sufficient to ensure uniform coverage of the skin surface, respectively. The receptor compartment was filled with 7.4 mL of PBS pH 7.4; the donor compartment was unoccluded. In separate experiments, the three formulations were applied for a period of either 6 or 12 h. During uptake, the cells were in an oven at 32°C. At the end of the application, the diffusion cell was disassembled and the residual formulation on the skin surface was removed using absorbent paper and alcohol wipes (70% isopropyl alcohol, FastAid pre-injection swabs; Robinson Healthcare, Worksop, UK). Approximately 25% of the treated skin area was then taken for immediate analysis by confocal Raman spectroscopy (see below).

After the 12-h uptake period only, the remaining portion of the skin was positioned on a 2% agar gel 'island' (prepared as previously described (Zarmpi et al., 2025)) floating in 20 mL of PBS in a petri dish and returned to the oven maintained at 32°C. Then, 2 and 4 h later, additional skin fractions (again, each about 25% of the original sample used) were sectioned and analysed by confocal Raman. These experiments permitted DOX clearance from the skin to be assessed from the results acquired at 0, 2 and 4 h (i.e., 12, 14 and 16 h, respectively, after the experiment began) post-termination of the 12-h uptake. To provide an internal control, the experiments with RLD-US were duplicated (and hereafter reported as RLD-US-R1 and RLD-US-R2). All experiments were performed in triplicate using skin acquired from three different pigs (resulting in n = 9 data points for each formulation, at each measurement time).

Table 1
Composition of the DOX formulations studied.

Formulation	DOX (%w/w)	Excipients
Commercial creams		
RLD-US[a]	5	sorbitol, cetyl alcohol, isopropyl myristate, glyceryl stearate, polyethylene glycol-1000 stearate, petrolatum, benzyl alcohol, titanium dioxide, purified water
Generic-US[b]	5	
Laboratory-made formulation		
90:10 v/v dodecanol/PG	8.2 (saturated)	dodecanol and propylene glycol (PG)

[a] Mylan Pharmaceuticals, 2017.
[b] Amneal Pharmaceuticals, 2023.

2.5. Confocal Raman spectroscopy

'Top-down' confocal Raman spectroscopy (Zarmpi et al., 2023) (Renishaw RM1000 Raman microscope running v4.4 WIRE software, Renishaw plc, Wotton-Under-Edge, UK) was employed to assess the disposition of DOX in the skin post-application of the formulations studied. The treated skin samples were mounted in a custom-built sample holder with an approximately 0.5 mL water-filled well to maintain tissue hydration (Zarmpi et al., 2023; Zarmpi et al., 2025). A diode laser (785 nm) with a 1200-line/mm grating provided spectral resolution of 1 cm^{-1}. As a calibration reference, a silicon wafer was used daily to correct for Raman frequency shifts or laser beam de-alignment by monitoring the frequency and intensity of the signal at 520 cm^{-1} (Zarmpi et al., 2023; Zarmpi et al., 2025).

Experimental spectra were acquired in the frequency range 663–1757 cm^{-1}, using a long, 50x working distance objective lens (NA = 0.90). To improve method sensitivity, most spectra were acquired using 80 accumulations (each of 20 s) and a laser power of 100%; exceptionally, the reference spectrum of solid DOX employed only ten 10-s accumulations to avoid signal saturation. Fig. 1 (left panels) shows the reference spectra of untreated skin, solid DOX, PG, dodecanol, the commercial gels and the laboratory-made solution.

DOX disposition in the skin was assessed by monitoring the C=C stretching vibration at 1605 cm^{-1}; PG and dodecanol were tracked via the C-O stretching at 840 cm^{-1} and CH_2 bending at 1448 cm^{-1}, respectively. The C=C stretching intensities at 1605 and 1634 cm^{-1} were sensitive to the physical state of the drug: the 1605 cm^{-1} signal had higher intensity than that at 1634 cm^{-1} when the drug is dissolved whereas, for the solid drug, the 1634 cm^{-1} signal was greater (Fig. 1, lower right panel)). The maximum intensity of phenyl ring breathing at 1003 cm^{-1} (often associated with phenylalanine (Pezzotti et al., 2015)) was recorded and used for normalisation (to account for attenuation and absorption of the infrared radiation by the skin (Zarmpi et al., 2025) of the target DOX, PG and dodecanol signals) as discussed further below; in this study, the Amide I vibration was not used because of its overlap with the adjacent DOX signal. Depth profiles were acquired at nominal depths of 5 μm and 25 μm from the skin surface at one specific location per sample, excluding skin 'crevices' and appendages. The selected depths were chosen, respectively, to provide measurements acquired

specifically from the stratum corneum (SC) and from the living epidermis below the barrier layer, based on literature in which porcine SC thickness was reported to be to be 8.5 ± 3.0 μm (n = 49) (Herkenne et al., 2006). The skin surface (0 μm) was determined by adjusting the focus of the confocal laser at minimal power (<5%) until clear topographical features were observed corresponding to a step-change in the of phenyl ring breathing signal at 1003 cm^{-1}. Spectra from untreated skin were also acquired from the three pig donors at both depths and in triplicate. All spectra were acquired using the LiveTrack™ feature to maintain focus (as precisely as possible) at the studied depths.

2.6. Treatment of confocal Raman data and critical level of detection

Baseline subtraction (Intelligent Fitting, v4.4 WIRE software) and cosmic ray removal (Width of Features detection wizard, v4.4 WIRE software) were performed on all acquired spectra. Signals of interest were then fitted (using the Curve Fit tool) and maximum intensities determined. Peaks have been consistently fitted around defined frequencies and maximum intensities at these specific frequencies are always reported. However, the fitting process can result in minor deviations of the maximum intensity from the specified frequency. This deviation is typically very small for sharp peaks (such as Phe) but may be slightly larger for broader or overlapping bands (such as Amide I).

The critical level of detection (A_c) was set as the standard deviation (SD) of the background noise in the fixed 1720–1755 cm^{-1} region (in which no drug or skin signals were expected) multiplied by 3. As described and justified elsewhere (Zarmpi et al., 2025), DOX, dodecanol and PG signal intensities lower than A_c were considered to be 'not accurately' determined and were replaced by $A_c/2$. The A_c value was determined for each measured spectrum, i.e., for each replicate experiment with each DOX formulation at each time and depth in each pig. In untreated skin samples (corresponding to the measurements reported at 0-h), the DOX, dodecanol and PG signals were assigned values of zero.

2.7. Bioequivalence between formulations and cutaneous pharmacokinetics assessed from confocal Raman data

For each pig donor, the arithmetic mean of the normalised intensities of the three replicates was calculated at each measurement time (6, 12, 14 and 16 h), depth (5 and 25 μm), and formulation. For each formulation and pig, the area under the normalised intensity versus time of measurement curve (AUC_t) was then determined (including zero at time = 0) using the trapezoidal rule. The arithmetic mean and standard deviation of the AUC_t values across pigs were then calculated for each formulation and depth.

To compare formulations, the AUC_t values were log-transformed, and within each pig, the difference in these values between each test formulation (i.e., generic and laboratory-made) and reference formulation (RLD-US-R1 or RLD-US-R2) was calculated at each depth. The arithmetic mean, standard deviation and upper and lower 90% confidence intervals (CIs) of these log-transformed differences across pigs were then determined. Finally, the antilogs of the means and 90% CIs were taken to obtain BE-like ratios for the test-to-reference formulations and the corresponding upper and lower 90% CIs.

First-order elimination rate constants (k_{elim}) describing DOX clearance into the deeper skin layers in each pig were determined from the arithmetic mean of the normalised intensities of the three replicates of each formulation at the 5 μm depth for each clearance time (0, 2 and 4 h). The natural log-transformed mean intensities were then plotted as a function of clearance time, and the deduced linear regression slopes (GraphPad Prism 5 (version 9.3.1, San Diego, CA)) yielded k_{elim} and its standard error for each formulation Statistically significant differences among formulations ($p < 0.05$) were evaluated using analysis of covariance (ANCOVA (Zar, 1984)) in GraphPad Prism.

2.8. Chromatographic analysis

Drug quantification in the solubility experiments used a modification of a previously published HPLC-UV method (Shimadzu LC-2010, Milton Keynes, UK) (Queiroz et al., 1995). Samples (20 μL) were injected onto a reversed-phase C18 column (HiQ sil C18HS C18 column 150 × 4.6 mm, 5 μm, Kromatek, Dunmow, UK) using an acetonitrile/acetate 0.25 N buffer pH 5.4 (60/40 v/v) as the mobile phase at 25°C. The flow rate was 1 mL min^{-1}, UV detection at 254 nm. The retention time was 6.2 min. Quantification was based on linear calibration curves of peak area versus concentration of standard DOX solutions (0.1–100 μg mL^{-1}) in MeOH. The limits of detection (LoD) and quantification (LoQ) were 0.02 and 0.07 μg mL^{-1}, respectively.

3. Results

3.1. Doxepin hydrochloride solubility

The solubilities of DOX in various solvents and solvent mixtures are presented in Table 2. It is noted that the equilibrium solubility of DOX in PBS at pH 7.4 was not quantified as even 5 g of the solid drug dissolved completely in 1 mL of the buffer to produce a clear solution with a pH of ~4.00. DOX was readily soluble in PG, PEG-400 and PEG-200, soluble in PEG-350 monomethyl ether, sparingly soluble in dodecanol, slightly soluble in oleic acid and practically insoluble in isopropyl myristate and isopropyl palmitate. In the solvent mixtures examined, solubilities were good, varied by around 3-fold from the smallest to the highest, and averaged around 140 mg mL^{-1}. The composition of the solvent mixtures was set at 90/10 v/v to avoid phase separation of the partially miscible components. Dodecanol/PG was chosen for the study because the saturation solubility of DOX therein was closest to the 5% w/w found in the tested creams.

3.2. Confocal Raman spectroscopy

Due to overlaps of both the DOX Raman signal at 1605 cm^{-1} and that from dodecanol at 1448 cm^{-1} with those from endogenous skin species, a signal separation strategy was implemented, based on the relative ratios of these signals to that of phenyl ring breathing at 1003 cm^{-1} (hereinafter assigned to phenylalanine (Phe)) in untreated skin, designated respectively as $I_{untreated\ skin,1605}/I_{untreated\ skin,1003}$ and $I_{untreated\ skin,1448}/I_{untreated\ skin,1003}$. Table 3 reports these ratios measured at nominal depths of 5 μm and 25 μm and Supplementary Table 1 provides the untreated skin intensity measurements at 1605, 1448 and 1003 cm^{-1} from which these ratios are derived. It is immediately apparent that these two sets of normalised values are similar at the two depths examined and that inter-pig variability is statistically non-significant (ANOVA).

Table 2
DOX solubilities in different solvents and solvent mixtures (mean ± SD, n = 3).

Solvents/*solvent mixtures*	Solubility (mg mL^{-1})	% w/w
PBS pH 7.4 (final pH ~ 4)[a]	>5000	>83.3%
PG	800 ± 300	43.6%
PEG-400	249 ± 49.3	18.1%
PEG-200	216 ± 60.9	16.1%
PEG-350 monomethyl ether	88.3 ± 12.6	7.5%
Dodecanol	14.2 ± 2.0	1.7%
Oleic acid	8.6 ± 0.4	0.95%
Isopropyl myristate	0.026 ± 0.002	0.003%
Isopropyl palmitate	0.018 ± 0.001	0.002%
PEG-200/dodecanol 90/10 v/v	*229 ± 69.2*	*17.3%*
PEG-350 monomethyl ether/PG 90/10 v/v	*159 ± 60.9*	*12.5%*
Oleic acid/PG 90/10 v/v	*101 ± 16.6*	*9.5%*
Dodecanol/PG 90/10 v/v	*76.3 ± 4.0*	*8.2%*

[a] PBS buffer composition: sodium chloride (137 mM), potassium chloride (2.7 mM), disodium phosphate dibasic (10 mM), monopotassium phosphate monobasic (1.8 mM).

Table 3
Normalised Raman signals (relative to that of phenyl ring breathing at 1003 cm^{-1} (typically associated with phenylalanine) from endogenous skin species at 1605 and 1448 cm^{-1} at nominal depths of 5 μm and 25 μm from three pigs (with 3 replicates per pig) together with the corresponding mean ± SD.

5 μm depth	$I_{untreated\ skin,1605}/I_{untreated\ skin,1003}$			$I_{untreated\ skin,1448}/I_{untreated\ skin,1003}$		
Pig donor	1	2	3	1	2	3
Replicate 1	0.144	0.143	0.148	1.26	1.02	1.12
Replicate 2	0.166	0.145	0.150	1.18	1.01	1.07
Replicate 3	0.129	0.126	0.145	1.15	1.17	1.02
Mean ± S.D.	0.146 ± 0.019	0.138 ± 0.010	0.148 ± 0.003	1.20 ± 0.06	1.07 ± 0.09	1.07 ± 0.05

25 μm depth	$I_{untreated\ skin,1605}/I_{untreated\ skin,1003}$			$I_{untreated\ skin,1448}/I_{untreated\ skin,1003}$		
Replicate 1	0.154	0.139	0.160	1.13	1.02	1.08
Replicate 2	0.187	0.154	0.149	1.03	0.98	1.01
Replicate 3	0.159	0.150	0.143	1.10	1.15	0.95
Mean ± S.D.	0.167 ± 0.018	0.148 ± 0.008	0.151 ± 0.009	1.09 ± 0.05	1.05 ± 0.09	1.01 ± 0.07

Knowing the Phe signal intensity in treated skin ($I_{treated\ skin,1003}$), as well as the $I_{untreated\ skin,1605}/I_{untreated\ skin,1003}$ and $I_{untreated\ skin,1448}/I_{untreated\ skin,1003}$ ratios in untreated skin, enables the intensity of endogenous skin species at 1605 and 1448 cm^{-1} in treated skin to be determined. This is then subtracted from the recorded maximum signals at these two frequencies, and the intensities of the unmixed signals of interest to be deduced. In this way, the unmixed DOX signal intensity at 1605 cm^{-1} ($I_{DOX,1605}$) in treated skin can be calculated from Eq. (1):

$$I_{DOX,1605} = I_{Total,1605} - \left(\frac{I_{untreated\ skin,1605}}{I_{untreated\ skin,1003}} \times I_{treated\ skin,1003}\right) \quad (1)$$

where $I_{Total,1605}$ is the measured maximum intensity at 1605 cm^{-1} in treated skin.

A similar strategy was employed to unmix the dodecanol (C12OH) signal from that of endogenous species in the skin at 1448 cm^{-1}. However, in this case, PG also contributes to the 1448 cm^{-1} total intensity (see Fig. 1). As a result, applying the calculation procedure of Eq. (1), as specified in Eq. (2), gives the unmixed intensities of dodecanol and PG combined at 1448 cm^{-1} ($I_{C12OH+PG,1448}$) in treated skin:

$$I_{C12OH+PG,1448} = I_{Total,1448} - \left(\frac{I_{untreated\ skin,1448}}{I_{untrested\ skin,1003}} \times I_{treated\ skin,1003}\right) \quad (2)$$

where $I_{Total,1448}$ is the measured maximum signal intensity at 1448 cm^{-1} in treated skin. Finally, the unmixed dodecanol signal at 1448 cm^{-1} ($I_{C12OH,1448}$) in treated skin was calculated using Eq. (3):

$$I_{C12OH,1448} = I_{C12OH+PG,1448} - \left(\frac{I_{PGref,1448}}{I_{PGref,840}} \times I_{treated\ skin,840}\right) \quad (3)$$

where $I_{PGref,1448}$ and $I_{PGref,840}$ are respectively the PG signal intensities at 1448 cm^{-1} and 840 cm^{-1} from the reference spectrum (see Fig. 1), and $I_{treated\ skin,840}$ is the signal intensity of PG at 840 cm^{-1} in treated skin. The unmixed DOX and unmixed dodecanol + PG signals were compared to the A_c to confirm that the active and inactive ingredients were accurately detected in the skin-treated experiments and then normalised by the corresponding Phe intensities.

The normalised DOX maximum intensities (relative to Phe) as functions of time and depth into the skin, for each pig skin 'donor', post application of the two commercial creams and the saturated solution in 90/10 v/v dodecanol/PG, are shown in Fig. 2. The 6- and 12-h measurements describe DOX uptake, those at 14 and 16 h characterise drug clearance (that is, at 2 and 4 h after the 12-h uptake). The 0-h data are measurements made before skin treatment and were therefore set to zero (as the skin had not, at this point, had any contact with the DOX formulations). Unmixed DOX maximum intensities below the A_c were replaced by $A_c/2$. The corresponding Phe maximum intensities for these experiments are presented in Supplementary Fig. 1.

The normalised DOX signal profiles generally demonstrated uptake and clearance phases although, for the cream products, this behaviour was less easily discerned due to the relatively low signals detected. Nonetheless, DOX was detectable typically to a nominal depth of 25 μm. As expected, attenuation of the DOX signal was observed (irrespective of the applied formulation) between 5 and 25 μm, consistent with the anticipated concentration gradient established. It was observed that the profiles from the RLD and generic creams were similar while that from the saturated dodecanol-PG solution clearly demonstrated enhanced drug delivery.

In skin treated with the laboratory-made saturated solution of dodecanol/PG 90/10 v/v, Raman signals from the two functional excipients were detected and the normalised intensities as a function of time and at nominal skin depths of 5 and 25 μm are shown in Fig. 3. No Raman signals from any of the inactive components of the reference and generic creams were measurable (data not shown). Post-application of the dodecanol/PG formulation, the latter co-solvent was detected, primarily during the 6- and 12-hr uptake periods, up to a depth of 25 μm depth; however, during clearance, the PG signals were small and often below the A_c. This absorption-elimination profile of PG is very similar to that reported previously from formulations of metronidazole (Zarmpi et al., 2025). In contrast, the cutaneous pharmacokinetics of dodecanol showed a more gradual uptake over 6–12 hr, rather than the more obvious maximum uptake of PG occurring at 6 hr.

3.3. Bioequivalence-like analysis of confocal Raman data

The areas under the normalised DOX signals as a function of time (AUC_ts) for each formulation at skin depths of 5 and 25 μm are in Table 4, and 'test'/RLD AUC_t ratios (and the corresponding 90% confidence intervals (CIs)) are in Table 5; the latter were calculated twice using both RLD-US-R1 and RLD-US-R2 as the reference formulation. The average 'test'/RLD ratios of the commercial creams all fell – regardless of skin depth or the choice of RLD-US replicate used – within the range 0.80–1.25, the criterion typically used in the assessment of bioequivalence ("*90% confidence interval of the ratio of a* log*-transformed exposure measure (*AUC_t *in this case) falls completely within the range 0.8–1.25"* (Schuirmann, 1987)). In contrast, the AUC_t ratios for the laboratory-made dodecanol/PG solution fell conclusively above this range. Unsurprisingly, however, given the limited number of replicates performed for the DOX cream products, the corresponding 90% CIs were never (if at all) fully within the BE limits, except for the comparison of Generic-US when RLD-US-R2 was used as the reference formulation.

3.4. Elimination rate constant of DOX from skin

Linear regressions of the natural logarithm of normalised DOX intensities as a function of clearance time for the formulations studied are shown in Fig. 4. At a nominal skin depth of 5 μm, the slopes can be considered to be the negative values of the first-order elimination rate constants (k_{elim}) of the drug from the upper skin layers, and these are

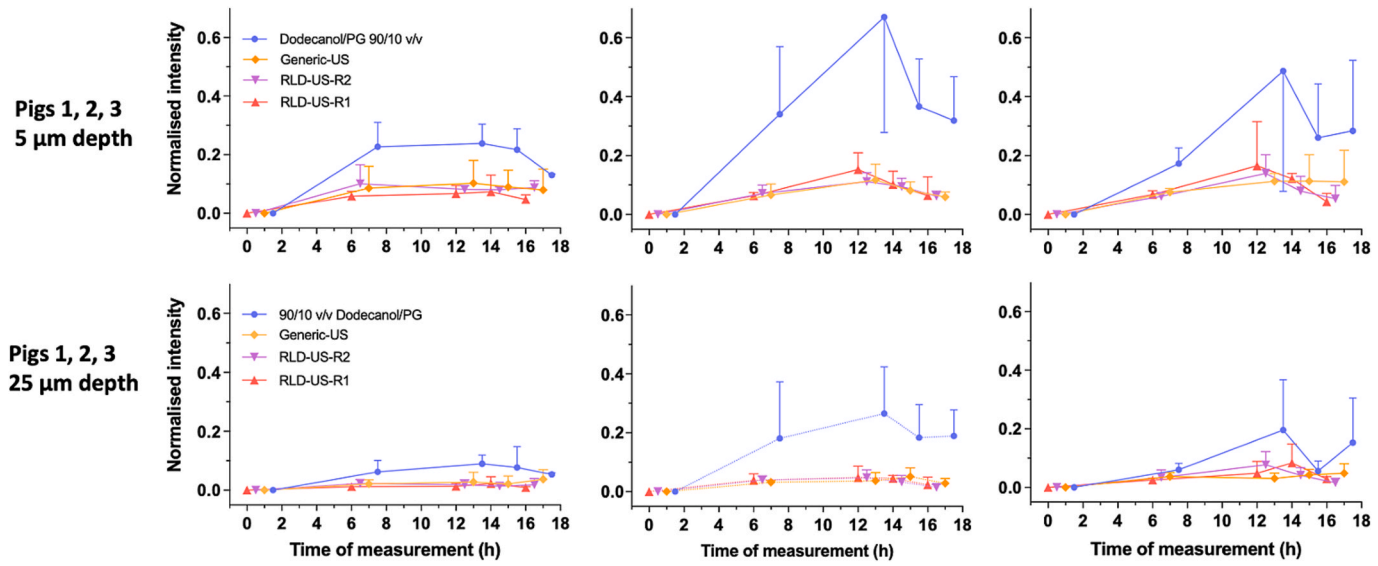

Fig. 2. Normalised DOX maximum intensities as a function of time at skin depths of 5 µm and 25 µm following application of the tested formulations to skin samples taken from pig donors 1, 2 and 3 (shown left to right). Data are the mean of the normalised intensities (with n = 3 replicates in each of the 3 pigs) + or − SD. For better visualization, some data points have been shifted slightly along the time-axis.

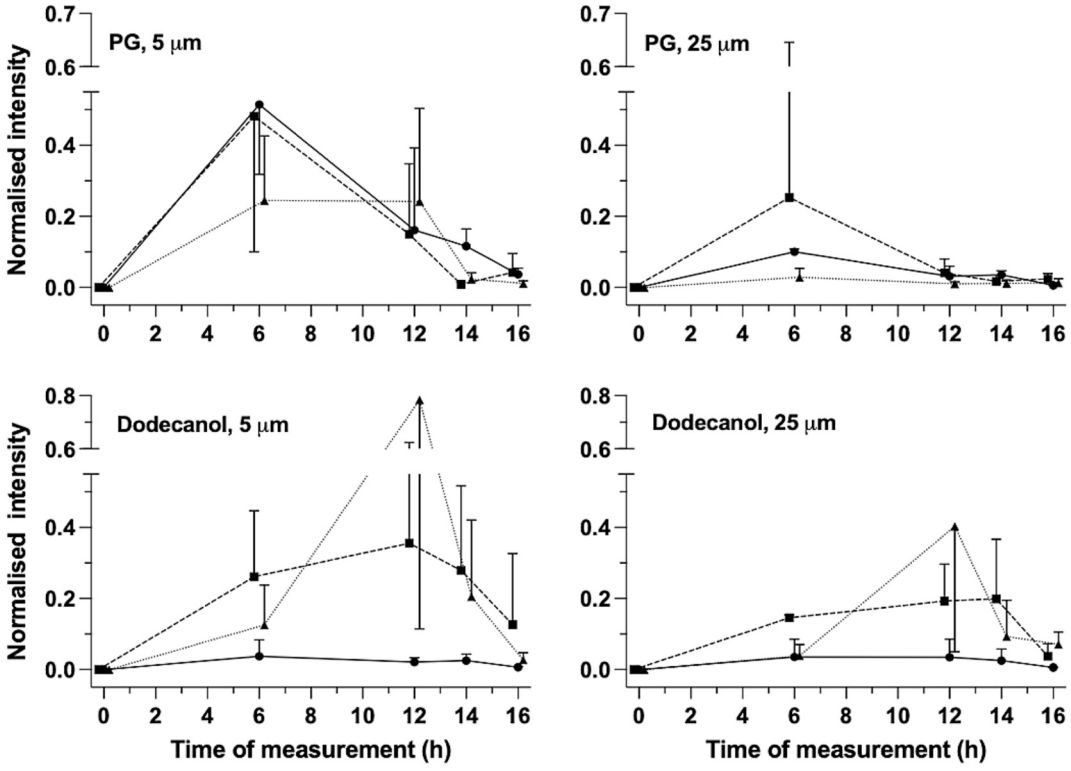

Fig. 3. Normalised PG and dodecanol maximum intensities as a function of time at skin depths of 5 µm and 25 µm following application of the laboratory-made formulation to skin samples taken from 3 different pig donors (the 3 profiles in the 4 graphs representing the data from the individual animals). Data are the mean of the normalised intensities (with n = 3 replicates in each of the 3 pigs) + or − SD. For better visualization, some data points have been shifted slightly along the x-axis.

reported in Table 6; ANOVA was unable to demonstrate any significant differences between these results. The pooled value of k_{elim} across all formulations was 0.14 h^{-1}.

4. Discussion

Although confocal Raman spectroscopy has been shown to be a potentially valuable tool with which to assess cutaneous drug BA and BE (or not) between topical products, it is unlikely to be universally applicable to all topical formulations. Differences in drug chemistry and the wide range of permeation rates through the skin, coupled with the complexity of typical dermatological formulations, can substantially impact on the resolution and sensitivity of the method. Nonetheless, previous studies (Maciel Tabosa et al., 2023; Zarmpi et al., 2023; Zarmpi

Table 4
DOX AUC_ts (h) determined from the data in Fig. 2 (mean ± SD of AUC_t for the 3 pigs calculated from the average normalised intensities (n = 3 replicates) at each time and depth (in each pig)).

Nominal depth into skin (μm)	Formulation			
	RLD-US-R1	RLD-US-R2	Generic-US	90/10 v/v Dodecanol/PG
5	1.14 ± 0.29	1.15 ± 0.03	1.17 ± 0.08	4.15 ± 1.48
25	0.42 ± 0.21	0.46 ± 0.18	0.42 ± 0.09	1.68 ± 0.91

Table 5
Mean BE AUCt ratios (±90% CIs) using either RLD-US-R1 or RLD-US-R2 as the 'reference' product at skin depths of 5 and 25 μm.

Reference product = RLD-US-R1, 5 μm depth			
Test product	BE ratio	Lower 90% CI	Upper 90% CI
RLD-US-R2	1.03	0.62	1.70
Generic-US	1.05	0.65	1.69
90/10 v/v Dodecanol/PG	3.57	2.35	5.41
Reference product = RLD-US-R1, 25 μm depth			
RLD-US-R2	1.14	0.81	1.61
Generic-US	1.11	0.57	2.19
90/10 v/v Dodecanol/PG	4.07	2.11	7.87
Reference product = RLD-US-R2, 5 μm depth			
RLD-US-R1	0.97	0.59	1.60
Generic-US	1.02	0.92	1.13
90/10 v/v Dodecanol/PG	3.47	1.85	6.49
Reference product = RLD-US-R2, 25 μm depth			
RLD-US-R1	0.87	0.62	1.23
Generic-US	0.97	0.65	1.45
90/10 v/v Dodecanol/PG	3.56	1.75	7.25

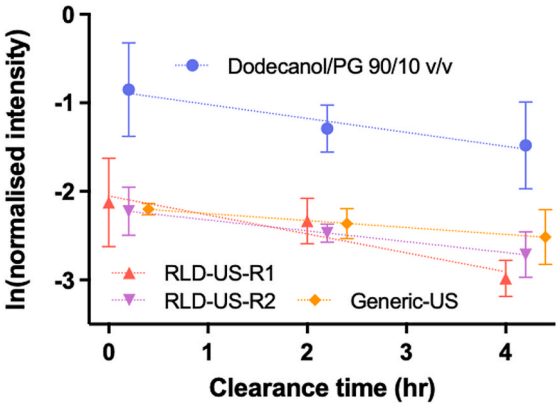

Fig. 4. First-order elimination of DOX post-application and removal of the formulations, measured at a nominal skin depth of 5 μm in 3 pig donors. The data points represent the pooled mean ± SD of the normalised intensities (means of three replicates per pig, averaged across the three animals). Lines are the best-fit linear regressions of the natural-log transformed within-pig mean values (one per pig) versus time. For better visualization, some data points have been shifted slightly along the time-axis.

et al., 2024) have laid a foundation for Raman as a useful method for further development and a recent investigation focused on MTZ gel products (Zarmpi et al., 2025) has produced encouraging results. It seems reasonable to expect, therefore, that further improvements in the technology will enable successful future assessment of a wider range of formulations.

Table 6
First-order elimination rate constants (k_{elim}) of DOX from the upper skin layers corresponding to the negative slope of the lines[a] plotted in Fig. 4 (mean ± SE; n = 3).

Test product	k_{elim} (h^{-1})
RLD-US-R1	0.21 ± 0.07
RLD-US-R2	0.12 ± 0.04
Generic-US	0.08 ± 0.04
90/10 v/v Dodecanol/PG	0.16 ± 0.08

[a] The slopes for the RLD replicates were significantly different from zero ($p < 0.05$), those for the generic product and the laboratory-made formulation were not; r^2 values for these slopes were 0.58, 0.55, 0.36 and 0.33, respectively, probably due (principally) to the clearance rates being slow enough that 4 h was not long enough to establish a statistically reliable slope.

In the current investigation, confocal Raman has been used to assess another dermatological active (DOX) applied to the skin in two complex topical cream products (the RLD and an approved generic) and in a laboratory-made solution formulation that was designed to be non-BE. Selection of the latter was made via a limited screening of DOX solubilities in a series of pure solvents and in a smaller number of 2-solvent mixtures (Table 2). The finally selected formulation was a 90/10 v/v mixture of dodecanol and PG, a combination of a solvent typically present in commercial products (i.e., PG), and another similar to typically present excipients (e.g., cetyl alcohol), that was anticipated to appreciably enhance DOX percutaneous permeation relative to that from the two creams.

Despite there being identifiably distinct DOX-related Raman signals – such as aromatic C═C stretching at 1605 cm^{-1} and 1615 cm^{-1}, C-O stretching at 1220 cm^{-1}, and aromatic out-of-plane C–H bending at 700 cm^{-1} (Fig. 1) – not all are suitable for tracking the drug's uptake and clearance from the skin. The promising-looking 1615 cm^{-1} signal unfortunately overlaps significantly with that of Amide I from keratin (making deconvolution and peak fitting difficult, if not impossible), that at 1220 cm^{-1} similarly aligns with those from endogenous skin species, and the 700 cm^{-1} signal is of insufficient intensity to be useful. Consequently, the 1605 cm^{-1} vibration, which overlaps less with Amide I than that at 1615 cm^{-1}, was selected to characterise the presence of DOX in the skin.[1]

When the confocal Raman approach described here was previously used to assess the relative cutaneous BA of 4-cyanophenol (Zarmpi et al., 2023) and metronidazole (Zarmpi et al., 2025), their selected vibrational signals were normalised with respect to that from the ubiquitous Amide I from the skin. For DOX, the proximity of the 1605 cm^{-1} aromatic C═C stretching to Amide I makes this approach untenable and the phenyl ring breathing motion (attributed to Phe) at 1003 cm^{-1} was used instead. The validity of this change has been demonstrated in untreated skin samples where the ratio of the Phe to Amide I signals is remarkably constant across pig skin donors and as a function of depth into the skin (Zarmpi et al., 2025). Of further value, as shown in this research, is that – again, in untreated skin – the intensity ratios, $I_{1605}/I_{Phe,1003}$ and $I_{1448}/I_{Phe,1003}$, are similarly consistent (Table 3) providing a path through which DOX and dodecanol signals can be effectively unmixed (including an additional step to correct for the contribution of PG to the dodecanol signal at 1448 cm^{-1}) from the endogenous skin background (Eqs. (1)–

[1] In terms of other components of the RLD and generic DOX creams, only benzyl alcohol may conceivably provide some interference with the drug's Raman spectrum. However, in its role as a preservative, this solvent is present at a relatively low level and its classification as a volatile organic solvent means that a significant fraction of that applied to the skin in a topical formulation is lost by evaporation rather than percutaneous penetration.

(3)). It should be noted that, although this signal separation strategy appears to be sensible and effective, background subtraction, instrument noise and calibration, intra/inter skin heterogeneity, and laser stability may introduce uncertainty in data analysis. The implementation of a more robust (i.e., less sensitive to spectral overlap) and automated approach is essential for future applications (particularly, *in vivo*). Other algorithms have been reported that are less sensitive to spectral overlap and permit the accuracy of skin penetration depth determination to be improved [Darvin, 2023].

DOX uptake into (at 6 h and 12 h) and clearance from the skin (2 h and 4 h after the 12 h uptake) was tracked at nominal skin depths of 5 μm and 25 μm, post-application of the formulations studied. The resulting absorption-elimination profiles are captured in Fig. 5. Analyses of these results in terms of areas under the normalised Raman signal versus time curves (AUC_t) are summarised in Tables 4 and 5. For the RLD and generic creams, the BE ratios all fall within the 0.80–1.25 acceptance criterion, regardless of which RLD-US repeat was used as the reference. However, because of the limited number of replicates performed and the variability typically associated with skin delivery measurements, the 90% confidence intervals unsurprisingly are not contained within the BE limits. As previously pointed out in the recent metronidazole investigation (Zarmpi et al., 2025), the number of replicates required to power a sufficiently sensitive protocol can be easily estimated. Nonetheless, the results are promising and validate the application of vibrational spectroscopy to assess BE not only for a broader range of drugs but also to complex topical products, such as creams.

The laboratory-made 90/10 dodecanol/PG solution was clearly differentiated from the marketed creams and the DOX AUC_t values at both skin depths indicated enhanced drug delivery relative to the RLD and generic creams (Table 4). The BE ratio of the solution AUC_t to either that of US-RLD-R1 or US-RLD-R2 was well above the 0.80 – 1.25 window and the 90% CIs did not overlap it at all (Table 5). In addition, it was possible to simultaneously track the disposition of both PG and dodecanol from the laboratory-made DOX solution (Fig. 3). The two profiles were quite distinct with PG being absorbed quickly into and through the skin (Nicoli et al., 2009) within 6 h, whereas dodecanol – consistent with its much more lipophilic character and its higher level in the solution both of which delay its depletion – exhibited a slower and more prolonged uptake that continued until the application was stopped at 12 h. The decent permeation of PG through the SC and into the underlying viable epidermis observed in this work is consistent with a number of reports in the literature (Bowen & Heard, 2006; Lopez-Dominguez et al., 2016; Thombre et al, 2020; Patel et al. 2021; Zarmpi et al., 2023, 2025).

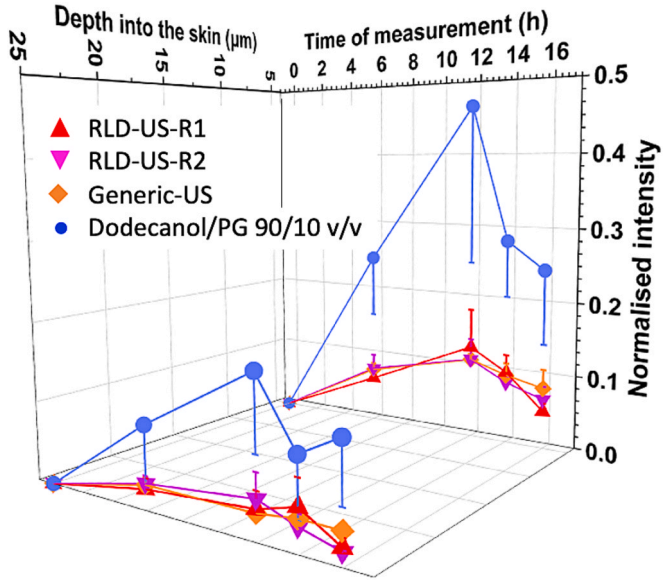

Fig. 5. Normalised DOX maximum intensities as functions of time of measurement and depth into the skin for the formulations studied. The combined and averaged data from three pig 'donors' are shown + or – S.D.

Additionally, the clearance data acquired at a nominal depth of 5 μm permitted a first-order elimination rate constant of DOX into the underlying skin tissue to be determined (Fig. 5). The results for the different formulations were not statistically distinguishable from one another suggesting that any impact of functional excipients on drug clearance had largely dissipated during this latter phase of the experiment (Pensado et al., 2019).

It is also appropriate to mention why only two depths were interrogated in the current work as compared to the recent publication (Zarmpi et al., 2025) using the same approach with metronidazole formulations where full depth profiles (at 5, 10, 15, 20, 25, and 35 μm) were acquired. First, in the metronidazole study, the scan time per depth was ~7 min (40 spectral accumulations of 10 s each), resulting in a total scan time of approximately 45 min per sample. To improve signal intensity in the current study (necessary due to the less efficient permeation of doxepin), 80 accumulations of 20 s were required meaning ~30 min per depth and about 1 h per sample. Given that skin dehydration increases significantly with increasing scan times, the acquisition of data at multiple depths would have been compromised by the loss of sample integrity. Second, a key objective of the present study was to evaluate whether a more limited tracking of drug disposition as functions of time and depth (focussing on two locations – one clearly in the stratum corneum, the other in the living epidermis, closer to the drug's site of action) would still enable useful conclusions about whether formulations are bioequivalent or not.

Finally, it is appropriate to place this research, and our recent work with confocal Raman and stimulated Raman spectroscopies, in the context of other contemporary findings with respect (a) to the assessment of cutaneous drug BA, and (b) to the potential of these approaches to contribute to the evaluation of BE between topical products. Over the last few years, there has been a noticeable increase in the use of vibrational spectroscopy in general to track the skin uptake of topically applied chemicals (Darvin, 2023). With improvements in available equipment and in the efficiency of signal collection and analysis, IR spectroscopic approaches, including Raman, have begun to focus more on the challenge of following the percutaneous absorption of drugs and other compounds of interest (including *inter alia* caffeine (Liu et al., 2021; Krombholz et al., 2022; Kourbaj et al., 2023), retinol (Krombholz et al., 2023), 4-cyanophenol (4-CP) and crisaborole (Maciel Tabosa et al., 2023; Zarmpi et al., 2024), diclofenac (Belsey et al., 2023), procaine (Binder et al., 2020), *trans*-retinol and propylene glycol (PG) (Caspers et al., 2019), metronidazole and PG (Zarmpi et al., 2025), ruxolitinib and deuterated betamethasone dipropionate (Feizpour et al., 2021), and tretinoin (Tu et al., 2025)) rather than investigating structural components of the skin and (for example) changes induced therein by hydration or functional excipients in topical formulations.

With respect to BE determination, confocal Raman is presently being subjected to increased scrutiny. In addition to the recent publication on metronidazole (Zarmpi et al., 2025), other *ex vivo* studies have been reported using comparable spectrophotometers and experimental designs: specifically, using a reference product as an internal control, incorporating a 'test' formulation deliberately chosen to be inequivalent to the reference (as in the present work), and monitoring, when possible, both the uptake of the active pharmaceutical ingredient (API) into/through the skin and its subsequent clearance.

A step-change has also taken place in terms of the use of *in vivo* confocal Raman spectroscopy, primarily enabled by the 'skin composition analyser' of RiverD International B.V. (Rotterdam, The Netherlands). Multiple publications using this equipment have appeared over more than decade demonstrating a number of applications in the pharmaceutical field and beyond. Most importantly with respect to the use of this approach as a regulatory tool for topical product BE

assessment, illustrative studies with ibuprofen (Iliopoulos et al., 2023) and salicylic acid (Link et al., 2025) have been carefully analysed to demonstrate future potential. In the same period, *ex vivo* methods based on confocal Raman measurements (typically employing spectrophotometers from either Renishaw plc (Wotton-Under-Edge, UK) or WiTec GmbH (Ulm, Germany)) on mammalian skin samples (human and porcine) have applied rigorous protocols to examine whether BE between different formulations of caffeine (Gaiser and Lunter, 2025a), ketoprofen (Gaiser and Lunter, 2025b), salicylic acid (Link et al., 2025) and metronidazole (Zarmpi et al., 2025) can be established. Another paper (Tu et al., 2025) has reported the bioequivalence evaluation of topical tretinoin formulations within human skin using stimulated Raman scattering (SRS) microscopy, focusing in particular on methodology to limit signal intensity variance due to the SRS system's performance, the different optical properties of cutaneous formulations, and the heterogeneity of light transmission through skin.

Nevertheless, and despite the evident progress with respect to the use of Raman, there remain areas where further improvement is required, and the outcomes desired from the approach – both *ex vivo* and *in vivo* – are made clearer. Among these issues (and in no particular order) are at least some of the following: Regulatory-level study design requirements must be standardised to at least some degree, and it should be acknowledged that they will mirror in some respects those that have been suggested for other approaches (e.g., IVPT, SC sampling) to topical product BE assessment. These include single dosing, positive and negative control formulations routinely used, the number and frequency of sampling times (uptake and clearance) to generate a kinetic profile identified, sample size calculation needed for a rigorous assessment of BE, and agreement on the appropriate cutaneous pharmacokinetic metrics to use. Next, for the determination of BE, it should be clarified whether Raman must provide absolute quantification of drug levels, as functions of time and position in the skin, if all products are to be tested on the same tissue/individuals. This is an important point as the development and validation of calibration methods with which to correlate spectroscopic signals to actual drug concentrations in different compartments of the skin is far from straightforward. As discussed in this article, and already in-depth in the literature, isolation of the drug's Raman signal from the potentially complex background due to endogenous skin components and formulation excipients requires further work on the unmixing algorithms/methods to ensure analytic sensitivity. More fundamentally, where should Raman measurements be made given that the definition of drug BA demands quantification of 'rate and extent' at or near the site of action? For topical products, the target may be the skin surface, the SC, living skin layers, or the appendages (e.g., follicles)… so which Raman approach (*ex vivo* or *in vivo*, confocal or SRS) is the most suitable for the different sites? Relatedly, the depth resolution, areas of skin that can be interrogated, and sensitivity of confocal Raman and SRS are different, as are their relative cost and accessibility; when will *in vivo* SRS be possible in humans and to what extent is laser power a limiting factor for SRS use on more pigmented skin? More positively, confocal Raman and SRS *ex vivo* have already been demonstrated to provide complementary topical product BE information to that generated by other methods, including IVPT and SC sampling. Lastly, right now, there is only one *in vivo* confocal Raman tool available commercially (from RiverD, the most recent iteration of which is its gen2-SCA: Skin Composition Analyzer) although there appears to be at least one other instrument on the horizon. Matching drug profiles across the SC has been largely successful (and far more elegant than SC sampling, of course) but validating drug quantitation progressively deeper into the skin appears to be a much greater challenge. Accessibility and capital outlay are other non-technical issues that also merit further consideration.

5. Conclusions

This research expanded the portfolio of confocal Raman spectroscopy in assessing non-invasively the disposition of topical drugs in the skin and demonstrating how the approach may ultimately permit the assessment of BE between RLD and generic products. Further to previously published work on metronidazole gels, it is now shown that the spectroscopic technique can track the disposition of DOX (a topical drug with Raman bands that significantly overlap with those from skin) from commercial creams which are often complex formulations that contain excipients that can interfere or mask the acquired spectra. A background signal removal strategy was employed to separate active, inactive and skin signals permitting the groundwork to be laid for automating the workflow and enabling more robust and scalable analyses in the future. The data enabled calculation of dermatopharmacokinetic metrics, including the AUC_t and a first-order elimination rate constant of the drug from the upper skin layers. Nonetheless, as observed before with metronidazole, the limited number of replicates and inherent variability in skin penetration restricted the generation of conclusive BE evaluations. It is without doubt that next steps should focus on developing a sound and statistically powered protocol to test the capabilities of this potentially valuable regulatory science tool *in vivo*.

CRediT authorship contribution statement

Panagiota Zarmpi: Writing – review & editing, Writing – original draft, Visualization, Methodology, Investigation, Formal analysis, Conceptualization. **Dimitrios Tsikritsis:** Writing – original draft, Visualization, Methodology, Investigation, Formal analysis, Conceptualization. **Natalie A. Belsey:** Writing – review & editing, Writing – original draft, Visualization, Methodology, Investigation, Formal analysis, Conceptualization. **Elena Rantou:** Writing – original draft, Validation, Methodology, Formal analysis. **Priyanka Ghosh:** Writing – review & editing, Writing – original draft, Project administration, Methodology, Investigation, Formal analysis, Conceptualization. **Annette L. Bunge:** Writing – review & editing, Writing – original draft, Validation, Methodology, Investigation, Formal analysis, Conceptualization. **Andrew C. Watson:** Writing – review & editing, Validation, Software, Methodology, Formal analysis. **Timothy J. Woodman:** Methodology, Validation, Writing - original draft. **M. Begoña Delgado-Charro:** Conceptualization, Investigation, Methodology, Validation, Writing – original draft, Writing – review & editing. **Richard H. Guy:** Conceptualization, Data curation, Formal analysis, Funding acquisition, Investigation, Methodology, Project administration, Supervision, Validation, Visualization, Writing – original draft, Writing – review & editing.

Declaration of competing interest

The authors declare the following financial interests/personal relationships which may be considered as potential competing interests: Richard Guy reports financial support was provided by Food and Drug Administration (FDA) of the U.S. Department of Health and Human Services (HHS). If there are other authors, they declare that they have no known competing financial interests or personal relationships that could have appeared to influence the work reported in this paper.

Acknowledgements

We dedicate this paper to Professor Joke Bouwstra in recognition of her incredibly rich and interdisciplinary research career and, specifically, her massive contributions to the fields of skin barrier function and topical/transdermal drug delivery. This project is supported by the Food and Drug Administration (FDA) of the U.S. Department of Health and Human Services (HHS) as part of a financial assistance award (1-U01-FD 006533) totalling $1.25M with 100% funded by FDA/HHS. The contents are those of the author(s) and do not necessarily represent the official views of, nor an endorsement, by FDA/HHS, or the U.S. Government. Valuable insight from and stimulating discussions with Drs. Sam Raney

and Markham Luke from the FDA's Office of Generic Drugs, and from Professor Jane White at the University of Bath, are gratefully acknowledged. NAB thanks the Community for Analytical Measurement Science for a 2020 CAMS Fellowship Award funded by the Analytical Chemistry Trust Fund.

Appendix A. Supplementary data

Supplementary data to this article can be found online at https://doi.org/10.1016/j.ijpharm.2026.126680.

Data availability

Data will be made available on request.

References

Amneal Pharmaceuticals, L. Doxepin Hydrochloride Cream, 5% – U.S. Prescribing Information. 2023. https://dailymed.nlm.nih.gov/dailymed/lookup.cfm?setid=dd8d5edd-7b08-4061-86e6-c4179da89c0d&utm_source=chatgpt.com (accessed 20 June 2025).

Belsey, N.A., Dexter, A., Vorng, J.-L., Tsikritsis, D., Nikula, C.J., Murta, T., Tiddia, M.V., Zhang, J., Gurdak, E., Trindade, G.F., et al., 2023. Visualisation of drug distribution in skin using correlative optical spectroscopy and mass spectrometry imaging. J. Control. Release 364, 79–89.

Binder, L., Valenta, C., Lunter, D., 2020. Determination of skin penetration profiles by confocal Raman microspectroscopy: evaluation of interindividual variability and interlab comparability. J. Raman Spectrosc. 51, 1037–1043.

Bowen, J.L., Heard, C.M., 2006. Film drying and complexation effects in the simultaneous skin permeation of Ketoprofen and propylene glycol from simple gel formulations. Int. J. Pharm. 307, 251–257.

Caspers, P.J., Nico, C., Bakker Schut, T.C., de Sterke, J., Pudney, P.D.A., Curto, P.R., Illand, A., Puppels, G.J., 2019. Method to Quantify the in vivo skin penetration of topically applied materials based on confocal Raman spectroscopy. Transl. Biophotonics 1, 1–10.

Darvin, M.E., 2023. Optical methods for non-invasive determination of skin penetration: current trends, advances, possibilities, prospects, and translation into *in vivo* human studies. Pharmaceutics 15, 2272.

Feizpour, A., Marstrand, T., Bastholm, L., Eirefelt, S., Evans, C.L., 2021. Label-free quantification of pharmacokinetics in skin with stimulated Raman scattering microscopy and deep learning. J. Invest. Dermatol. 141, 395–403.

Food & Drug Administration (FDA). Generic Drug Research - Related Guidances and Reports. 2025. https://www.fda.gov/drugs/generic-drugs/generic-drug-research-related-guidances-reports?utm_campaign=CDER%20New%201/3&utm_medium=email&utm_source=Eloqua&elqTrackId=37c218c5d2c94d5cac2e43f324e55012&elq=319215e068e94e79a9c3e8398b23d42d&elqaid=1946&elqat=1&elqCampaignId=1314 (accessed 09 September 2025).

European Medicines Agency (EMA). Guideline on quality and equivalence of locally applied, locally acting cutaneous products. EMA/CHMP/QWP/708282/2018 (adopted on 9 September 2024 by the Committee for Medicinal Products for Human Use (CHMP)); effective from 2 April 2025.

Gaiser, A., Lunter, D., 2025a. Advanced investigation of the suitability of Confocal Raman spectroscopy for dermatological bioequivalence assessments using caffeine and 1,2-pentanediol. Eur. J. Pharm. Sci. 215, 107324.

Gaiser, A., Lunter, D., 2025b. Investigation of the suitability of confocal Raman spectroscopy for the demonstration of bioequivalence of topical products. Int. J. Pharm. 671, 125214.

Ghosh, P., Raney, S.G., Luke, M.C., 2022. How does the food and drug administration approve topical generic drugs applied to the skin? Dermatol. Clin. 40, 279–287.

Herkenne, C., Naik, A., Kalia, Y.N., Hadgraft, J., Guy, R.H., 2006. Pig ear skin *ex vivo* as a model for *in vivo* dermatopharmacokinetic studies in man. J. Pharm. Res. 23, 1850–1856.

Herkenne, C., Naik, A., Kalia, Y.N., Hadgraft, J., Guy, R.H., 2008. Effect of propylene glycol on ibuprofen absorption into human skin *in vivo*. J. Pharm. Sci. 97, 185–197.

Iliopoulos, F., Caspers, P.J., Puppels, G.J., Lane, M.E., 2020. Franz cell diffusion testing and quantitative confocal Raman spectroscopy: *in vitro – in vivo* correlation. Pharmaceutics 12, 887.

Iliopoulos, F., Tang, C.F., Li, Z., Rahma, A., Lane, M.E., 2023. Confocal Raman spectroscopy for assessing bioequivalence of topical formulations. Pharmaceutics 15, 1075.

Iliopoulos, F., Tu, D., Pence, I.J., Li, X., Ghosh, P., Luke, M.C., Raney, S.G., Rantou, E., Evans, C.L., 2024. Determining topical product bioequivalence with stimulated Raman scattering microscopy. J. Control. Release 367, 864–876.

Jung, N., Namjoshi, S., Mohammed, Y., Grice, J.E., Benson, H.A.E., Raney, S.G., Roberts, M.S., Windbergs, M., 2022. Application of confocal Raman microscopy for the characterization of topical semisolid formulations and their penetration into human skin *ex vivo*. Pharm. Res. 39, 935–948.

Kourbaj, G., Gaiser, A., Bielfeldt, S., Lunter, D., 2023. Assessment of penetration and permeation of caffeine by confocal Raman spectroscopy *in vivo* and *ex vivo* by tape stripping. Int. J. Cosmet. Sci. 45, 14–28.

Krombholz, R., Fressle, S., Lunter, D., 2023. *Ex vivo—in vivo* correlation of retinol stratum Corneum penetration studies by confocal Raman microspectroscopy and tape stripping. Int. J. Cosmet. Sci. 44, 299–308.

Krombholz, R., Fressle, S., Nikolić, I., Pantelić, I., Savić, S., Sakač, M.C., Lunter, D., 2022. *Ex vivo—in vivo* comparison of drug penetration analysis by confocal Raman microspectroscopy and tape stripping. Exp. Dermatol. 31, 1908–1919.

Link, J., Heusel, C., Lunter, D.J., 2025. A pivotal, dermal, *in-vivo* bioequivalence study performed by confocal Raman spectroscopy (CRS). Eur. J. Pharm. Biopharm. 217, 114891.

Liu, Y., Krombholz, R., Lunter, D.J., 2021. Critical parameters for accurate monitoring of caffeine penetration in porcine skin using confocal Raman spectroscopy. Int. J. Pharm. 607, 121055.

Lopez-Dominguez, V., Boix-Montañes, A., Redo-Sanchez, A., Tejada-Palacios, J., 2016. Direct estimation of the permeation of topical excipients through artificial membranes and human skin with non-invasive terahertz time-domain techniques. J. Pharm. Pharmacol. 68, 873–882.

Maciel Tabosa, M.A., Cordery, S.F., White, K.A.J., Bunge, A.L., Guy, R.H., Delgado-Charro, M.B., 2022. Skin pharmacokinetics of diclofenac and co-delivered functional excipients. Int. J. Pharm. 614, 121469.

Maciel Tabosa, M.A., Vitry, P., Zarmpi, P., Bunge, A.L., Belsey, N.A., Tsikritsis, D., Woodman, T.J., White, K.A.J., Delgado-Charro, M.B., Guy, R.H., 2023. Quantification of chemical uptake into the skin by vibrational spectroscopies and stratum Corneum sampling. Mol. Pharm. 20, 2527–2535.

Mylan Pharmaceuticals, I. Doxepin Hydrochloride Cream, 5% – U.S. Prescribing Information. 2017. https://dailymed.nlm.nih.gov/dailymed/drugInfo.cfm?setid=b4771ea7-c19b-4182-bb23-c1473ab583fa (accessed 20 June 2025).

Nico, C., Bakker Schut, T.C., Caspers, P.J., Puppels, G.J., 2024. Limits of detection of topically applied products in the skin using *in vivo* Raman spectroscopy. Pharmaceutics 16, 304.

Nicoli, S., Bunge, A.L., Delgado-Charro, M.B., Guy, R.H., 2009. Dermatopharmacokinetics: factors influencing drug clearance from the stratum corneum. Pharm. Res. 26, 865–871.

OECD (Organisation for Economic Co-operation & Development). Test No. 105: Water Solubility, OECD Guidelines for Testing of Chemicals, Section 1. 1995. https://www.oecd.org/en/publications/test-no-105-water-solubility_9789264069589-en.html (accessed 05 March 2025).

Patel, A., Iliopoulos, F., Caspers, P.J., Puppels, G.J., Lane, M.E., 2021. *In vitro-in vivo* correlation in dermal delivery: the role of excipients. Pharmaceutics 13, 542.

Pensado, A., Chiu, W.S., Cordery, S.F., Rantou, E., Bunge, A.L., Delgado-Charro, M.B., Guy, R.H., 2019. Stratum corneum sampling to assess bioequivalence between topical acyclovir products. Pharm. Res. 36, 1–16.

Pezzotti, G., Boffelli, M., Miyamori, D., Uemura, T., Marunaka, Y., Zhu, W., Ikegaya, H., 2015. Raman spectroscopy of human skin: looking for a quantitative algorithm to reliably estimate human age. J. Biomed. Opt. 20, 065008.

Pot, L.M., Coenraads, P.J., Blömeke, B., Puppels, G.J., Caspers, P.J., 2016. Real-time detection of p-phenylenediamine penetration into human skin by *in vivo* Raman spectroscopy. Contact Dermatitis 74, 152–158.

Queiroz, R.H., Lanchote, V.L., Bonato, P.S., de Carvalho, D., 1995. Simultaneous HPLC analysis of tricyclic antidepressants and metabolites in plasma samples. Pharm. Acta Helv. 70, 181–186.

Raney, S.G., Ghosh, P., Ramezanli, T., Lehman, P.A., Franz, T.J., 2022. Cutaneous pharmacokinetic approaches to compare bioavailability and/or bioequivalence for topical drug products. Dermatol. Clin. 40, 319–332.

Raney, S.G., Luke, M.C., 2020. A new paradigm for topical generic drug products: impact on therapeutic access. J. Am. Acad. Dermatol. 82, 1570–1571.

Schuirmann, D.J.A., 1987. Comparison of the two one-sided tests procedure and the power approach for assessing the equivalence of average bioavailability. J. Pharmacokinet. Biopharm. 15, 657–680.

Thombre, A., Tse, S., Yeoh, T., Chen, R., North, R., Brown, M., 2020. *Ex vivo* (human skin) and *in vivo* (minipig) permeation of propylene glycol applied as topical crisaborole ointment. Int. J. Pharm. 576, 118847.

Tu, D., Lemberger, N.S., Wallmeier, K., Riseman, J., Kuzma, B.A., Wei, Y., Khoo, T.C., Rantou, E., Ghosh, P., Luke, M.C., Raney, S.G., Fallnich, C., Evans, C.L., 2025. Improved dual-modality bioequivalence evaluation of topical formulations within human skin using stimulated Raman scattering microscopy. Pharmaceutics 17, 1193.

Zar, J.H., 1984. Biostatistical Analysis. Prentice-Hall Inc, Englewood Cliffs.

Zarmpi, P., Maciel Tabosa, M.A., Vitry, P., Bunge, A.L., Belsey, N.A., Tsikritsis, D., Woodman, T.J., Delgado-Charro, M.B., Guy, R.H., 2023. Confocal Raman spectroscopic characterization of dermatopharmacokinetics *ex vivo*. Mol. Pharm. 20, 5910–5920.

Zarmpi, P., Tsikritsis, D., Vorng, J.-L., Belsey, N.A., Bunge, A.L., Woodman, T.J., Delgado-Charro, M.B., Guy, R.H., 2024. Evaluation of chemical disposition in skin by stimulated Raman scattering microscopy. J. Control. Release 368, 797–807.

Zarmpi, P., Tsikritsis, D., Watson, A.C., Vorng, J.-L., Tyagi, V., Belsey, N.A., Rantou, E., Ghosh, P., Bunge, A.L., Woodman, T.J., et al., 2025. Raman spectroscopy as a tool to accelerate development of complex medicinal products. J. Control. Release, 114190.